Thermochimica Acta 617 (2015) 200–207

Contents lists available at ScienceDirect

Thermochimica Acta

journal homepage: www.elsevier.com/locate/tca

# Experimental evidence for two distinct deeply supercooled liquid states of water – Response to "Comment on 'Water's second glass transition'", by G.P. Johari, Thermochim. Acta (2015)

J. Stern[a,1], M. Seidl[a,1], C. Gainaru[b,1], V. Fuentes-Landete[a], K. Amann-Winkel[a,2], P.H. Handle[a], K.W. Köster[b], H. Nelson[b], R. Böhmer[b,*], T. Loerting[a,*]

[a] Institute of Physical Chemistry, University of Innsbruck, 6020 Innsbruck, Austria
[b] Fakultät Physik, Technische Universität Dortmund, 44221 Dortmund, Germany

ARTICLE INFO

*Article history:*
Received 23 December 2014
Received in revised form 19 August 2015
Accepted 22 August 2015
Available online 2 September 2015

*Keywords:*
Amorphous ices
Polyamorphism
Glass transitions
Deeply supercooled liquid water
Metastability
Differential scanning calorimetry
Dielectric relaxation spectroscopy

ABSTRACT

Recently, our earlier data which led us to conclude that deeply supercooled water displays a second glass transition (Amann-Winkel et al., 2013) was reinterpreted (Johari, 2015). In particular, the increase in heat capacity observed for high-density amorphous ice (HDA) samples at 116 K was reinterpreted to indicate sub-$T_g$ features of low-density amorphous ice's (LDA's) glass transition. We reply to the criticism in detail and report an experiment triggered by the comment on our work. This experiment unequivocally confirms our original interpretation of the observations and reinforces the case for water's second glass transition, its polyamorphism, and the observation of two distinct ultraviscous states of water differing by about 25% in density.



## 1. Brief introduction

Recently, we reported on a series of calorimetric and dielectric experiments carried out for high-density amorphous ice (HDA) and low-density amorphous ice (LDA) which led us to conclude that water displays two distinct glass transitions [1] linking the two amorphous ices to two distinct ultraviscous liquid states. In a subsequent contribution G.P. Johari [2] suggests a reinterpretation of our findings [1]. In particular, he suggests to reinterpret the increase in heat capacity $\Delta C_{p,2} = 4.8\,J\,K^{-1}\,mol^{-1}$ observed at 116 K upon heating a sample of expanded high-density amorphous ice (eHDA) at ambient pressure. We note that recent theoretical work advances yet another interpretation of our results, involving two amorphous ices and facile crystallization of a single liquid [3].

In the comment [2], on which we respond in the present article, it is proposed that our observations, instead of being viewed as the signature of eHDA's glass transition, need to be interpreted as a sub-$T_g$ endotherm of LDA, whose $T_{g,1}$ is 136 K [4,5]. Ideas of a sub-$T_g$ nature of LDA's heat capacity increase at $T_{g,1} = 136$ K were proposed in the past, with the implication that the real $T_g$ of the low-density liquid (LDL) related to LDA would be above the crystallization temperature and thus experimentally unobservable [6,7]. These ideas were then scrutinized, vindicating the original interpretation that for LDA a glass transition occurs below its crystallization temperature [8,9]. Whether this glass transition is a glass-to-liquid transition or an orientational glass transition, is a separate matter on which consensus has not been reached so far [10,11]. Nevertheless, for LDA a glass-to-liquid transition is not questioned in Ref. [2] as exemplified by the quote: "water at $T > 136$ K is an ultraviscous liquid that crystallizes, and not a glass".

Here we focus our attention on the question raised by Johari whether our recent experiments can be reconciled with a single glass transition scenario or whether they indicate two distinct glass transitions. First, we review several important aspects regarding the transitions among water's high- and low-density forms and then move on to report a novel experiment inspired by the discourse. This experiment is designed to be capable of deciding between the two scenarios. Ultimately, the observations we make exclude the interpretation given in Ref. [2].

* Corresponding authors.
*E-mail addresses:* roland.bohmer@tu-dortmund.de (R. Böhmer), thomas.loerting@uibk.ac.at (T. Loerting).
[1] These authors contributed equally to the work.
[2] Current address: Fysikum, Stockholm University, 106 91 Stockholm, Sweden.

http://dx.doi.org/10.1016/j.tca.2015.08.030
0040-6031/

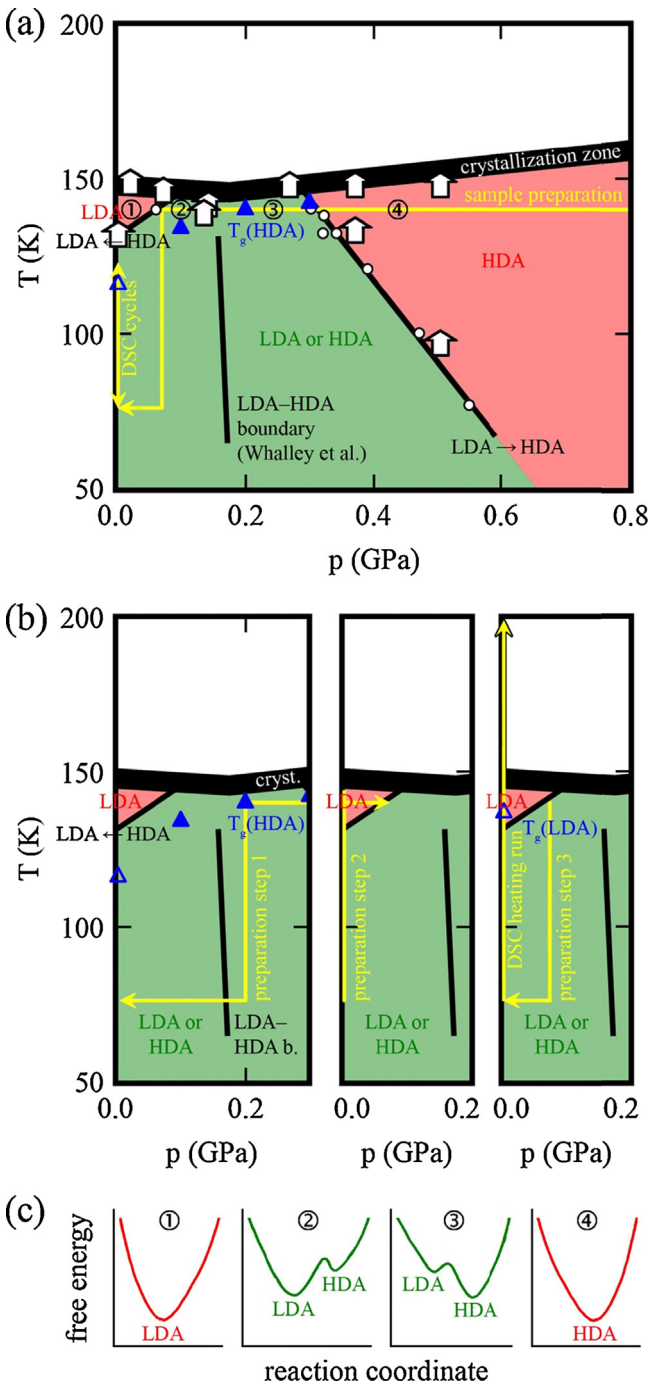


**Fig. 1.** (a) "Phase diagram" of the amorphous ices LDA and HDA. The word "phase diagram" is put in quotes here because, as explained in the text, not all states appearing in this diagram are necessarily phases in the thermodynamic sense. The area in green (labeled 2 and 3) shows p–T conditions, in which either LDA or HDA can be kept and studied for long times. Whether LDA or HDA is observed in experiments depends on the path of preparation. The two areas in red show p–T conditions, in which HDA transforms rapidly to LDA (red area labeled 1) and in which LDA transforms rapidly to HDA (red area labeled 4). The LDA-HDA boundary labeled "(Whalley et al.)" divides the green area and shows the location of equal free energy for HDA and LDA [22,23]. White circles and white arrows indicate the location of the sharp polyamorphic transition observed in isothermal and isobaric experiments, respectively. HDA → LDA transformation temperatures were taken from Refs. [19] and [1]. LDA → HDA transition and crystallization temperatures were taken from Ref. [12]. The open blue triangle indicates the calorimetric glass transition for HDA at 116 K [1], and filled blue triangles indicate volumetric glass transition temperatures for HDA [25]. In the white area above the thick black line labeled "crystallization zone" only crystalline ices can be observed at long time scales. The yellow arrow labeled "sample preparation" indicates the path taken in Ref. [1] for preparing those HDA sample that were subsequently studied by DSC and dielectric experiments at ambient pressure. The double-headed arrow labeled "DSC cycles" indicates that HDA samples were cycled in the DSC experiments between 77 and 123 K without observing a transformation to LDA. (b) Schematic route of preparation of LDA-II. The first part illustrates the decompression of VHDA from 1.10 to 0.20 GPa yielding eHDA, which is then quenched and subsequently decompressed to 0.002 GPa. In the second part eHDA is heated at 0.002 GPa–145 K and then compressed to 0.07 GPa where it is equilibrated for 60 s. Subsequently, the sample is quenched to 77 K and then decompressed to ambient pressure for ex situ DSC measurements as shown in part 3. (c) Sketch of Gibbs free energies of amorphous ices as a function of pressure. In the red area labeled ① LDA is the most stable amorphous form, and in the red area labeled ④ HDA is the most stable amorphous form. HDA is instable in area ① and LDA is instable in area ④, and so single-well Gibbs free energies result. In the green area labeled ② LDA is the most stable amorphous ice, and in the green area labeled ③ HDA is the most stable amorphous ice. At about 0.20 GPa LDA and HDA are of equal Gibbs free energy, which is the basis of the line labeled "Whalley et al." in (a). To the left of this line (green area ② ) HDA is metastable (rather than instable) with respect to LDA, whereas to the right of this line (green area ③ ) LDA is metastable with respect to HDA. That is, in the green area the Gibbs free energies show a double-well nature and an energy barrier, which cannot be surmounted on the basis of the available thermal energy. These two "megabasins" are at the origin of water polyamorphism, water's two glass transitions and the two deeply supercooled liquid forms LDL and HDL. Part (a) and (b) are adapted from [12]. (For interpretation of the references to color in figure legend, the reader is referred to the web version of the article.)

## 2. Pressure-induced transitions between HDA and LDA

Not only based on the experiments to be reported below but also based on the following arguments our initial interpretation is reconfirmed. Fig. 1(a) shows the transformation behavior of amorphous ices established by Mishima in 1994 [12]. The key feature of this diagram is the large hysteresis between the HDA → LDA and LDA → HDA transitions. As a result, there is a region in the diagram, in which amorphous ice appears exclusively as LDA (red area labeled ① in Fig. 1(a)), a region, in which amorphous ice appears exclusively as HDA (red area labeled ④ in Fig. 1(a)) and a region, in which either LDA or HDA may persist (green area labeled ② and ③ in Fig. 1(a)). Whether the thermodynamically more stable form or the metastable form exists within the green area in Fig. 1(a) depends on the pressure–temperature path taken in the course of the experiment. The polyamorphic transitions are very sharp and rapid both for the LDA → HDA and for the HDA → LDA [12] transitions and both for isothermal (circles in Fig. 1(a)) and for isobaric experiments (vertical arrows in Fig. 1(a)) at the locus of the transformation (black lines separating red and green areas in Fig. 1(a)). At pressures and temperatures away from the transformation boundaries, well inside the colored areas, transformations between LDA and HDA cannot be observed on the laboratory time scale of many hours [12–14].

Instead of the polyamorphic transition, the HDA-matrix relaxes upon keeping the sample at high temperatures close to the crystallization temperature for a while. Unannealed HDA (uHDA) [15] slowly relaxes, e.g., at 0.2 GPa and converges to an expanded HDA (eHDA) state [16], which we regard to be an equilibrated form of HDA, if prepared properly [14]. Furthermore, eHDA is highly stable and resistant against crystallization [17,18]. The eHDA sample studied in our earlier work [1] was prepared by decompression of a VHDA sample at 140 K, i.e., by entering the green area ② in Fig. 1(a) coming from the high-pressure, HDA side (area ④ ). The yellow arrow labeled "sample preparation" in Fig. 1(a) indicates the p–T path taken to prepare the sample used in Ref. [1]. We have taken care to avoid the HDA → LDA transition by quenching the sample just prior to entering the red LDA area ① in Fig. 1(a), i.e., by quenching the sample at 0.07 GPa from 140 K to 77 K, and then by releasing the pressure at 77 K [14,19]. The volume of the sample was monitored in situ by recording the piston displacement and did not show the jump-like change typical of the HDA → LDA transition. Thus, this procedure results in a sample of eHDA. The sample

was then characterized at ambient pressure using a range of methods, including powder X-ray diffraction, cryoflotation, and Raman spectroscopy (see below). These methods showed that the sample has a density of 1.13 g/cm$^3$ [20] and displayed a halo peak in X-ray diffractograms characteristic of HDA, with the halo maximum at $2\theta \approx 29^\circ$ (Cu-$K_{\alpha,1}$ radiation) [14,19].

The eHDA sample was subsequently studied by differential scanning calorimetry (DSC) at ambient pressure. Upon heating eHDA repeatedly to 116 K < $T$ < 130 K at ambient pressure (see double-headed, yellow arrow labeled "DSC cycles" in Fig. 1(a)) [1], it remains in its high-density state as the jump-like change to the LDA state is avoided (see boundary between the red and green areas ① and ② at ambient pressure in Fig. 1(a)). When heating eHDA samples at ambient pressure their volume increases suddenly by about 25% above 130 K [14–16]. Since the jump-like polyamorphic transition releases latent heat, the transition temperature can be detected also as a very sharp exotherm in DSC experiments [14]. Such an exotherm was found near 132 K, see trace 3 in Fig. 2 of Ref. [1] which is reproduced as Fig. 1 in the comment [2]. Johari suggests to view this massive exotherm as indicating a minimum which otherwise appears as a sub-$T_g$ effect in pressure-densified glasses such as polystyrene [2]. We emphasize that $C_p$ minima in such glasses are known to be usually very shallow (as is also evident from Fig. 2 of Ref. [2] which reproduces corresponding data for polystyrene), whereas for the amorphous ices we study the $C_p$ minimum is very deep. In the example of polystyrene shown by Johari the ratio of $C_p$ increase to the maximum and the $C_p$ decrease to the minimum is about 1:1. In previous observations on HDA [1] and LDA [4,5,21] this ratio is on the order of 1:1000. A similar ratio is also found in the present work – see Section 5, below. The ratio strongly depends on the heating rate and strongly decreases with increasing heating rate. In our observations it is reduced by half when increasing the heating rate in the calorimetry experiment from 10 K/min to 30 K/min. This is typical of latent heat peaks, but inconsistent with the idea of a mere change of heat capacity, which would be the case for sub-$T_g$ features. In fact, the ratio needs to be insensitive to changes in heating rate in case of a change of heat capacity. Pressure-densified glassy materials also do not show jump-like changes in volume at the temperature of the minimum (see references provided in [2]), by contrast to the observations made on amorphous ices.

In our earlier experiments [1] the onset of the glass transition at 116 K, thus, clearly pertains to a sample in its high-density state, but not to a sample in a lower-density state as suggested in Ref. [2] by comparison with pressure-densified polystyrene. The relevant difference between glassy polystyrene and glassy water is that only water shows polyamorphism, which manifests itself in the hysteresis and jump-like amorphous-amorphous transitions as implied by Fig. 1(a). The basis for this polyamorphism is the possibility of keeping HDA metastable for long times in the p,T-field ②, in which LDA is thermodynamically favored over HDA, and the possibility of keeping LDA metastable for long times in the p,T-field ③, in which HDA is favored over LDA (see Fig. 1(c)).

In Ref. [2] it is stated that "Thermodynamics requires that the LDA and HDA be at equilibrium at these 'phase boundaries', and ... a small increase in p or T ... would cause the transformation to occur in one direction and decrease in p or T thereafter would cause the transformation to occur in the opposite direction. But this reversibility has not been observed." [1]. Put this way this statement challenges the concept of polyamorphism established by Whalley et al. [22,23] and sketched in Fig. 1. Certainly, a phase boundary in a phase diagram implies equality of Gibbs free energies for two phases, where one phase is more stable on one side and the other is more stable on the other side of the phase boundary. We agree with Whalley et al. [22,23] and it is also pointed out in the comment [2] that the two lines separating the green areas ② and ③ from the two red areas ① and ④ do not reflect phase boundaries that are determined by thermodynamics. The requirements of thermodynamics often do not play the key role at low temperature, but instead kinetics takes over. With thermodynamic equilibrium established at ambient pressure water would freeze at 0 °C, but in fact supercooling is very often observed, e.g., in cloud droplets [24]. Even though equilibrium thermodynamics indicates equality of melting and freezing points, in reality the freezing point is often much below the melting point. A similar situation is encountered for LDA and HDA: LDA can be overpressurized and exist at p–T conditions ③, in which thermodynamics would favor HDA to exist, and similarly HDA can exist at p–T conditions ②, in which thermodynamics would favor LDA to exist. The green areas ② and ③ in Fig. 1(a) show the domains, in which thermodynamic requirements do not dictate what is experimentally observed, but in which kinetic hindrance results in a hysteresis between the upstroke LDA → HDA and the downstroke HDA → LDA transitions. In terms of a potential energy landscape picture this kinetic hindrance can be thought of as an energy barrier preventing the conversion to lower-lying states (see Fig. 1(c)). In this sense the potential energy landscape and megabasin concepts are useful and applicable for understanding our experiments and the nature of the high-density liquid at 0.1 MPa at $T > T_{g,2}$ = 116 K, although they do not reveal the details of the molecular processes.

## 3. Why HDL is not just pressure-densified water

Furthermore, in Ref. [2] it is argued that at 0.07 GPa and 140 K our sample is above its volumetric glass transition temperature [25] (see blue triangles in Fig. 1(a)), thus presumably in its liquid state. Johari suggests that upon quenching to 77 K the sample transforms to "*pressure-densified glassy water*". This supposition implies conversion of HDA to LDA slightly above the volumetric glass transition at 0.07 GPa. In fact, it would need to adopt the same state that LDA water adopts when pressurized from ambient pressure to 0.07 GPa. However, our previous observations revealed that signs of a transformation from a high-density to a low-density state at 0.07 GPa and 140 K cannot be detected. The characteristic OH-stretching bands for HDA and for LDA are well separated [26], and so transformation to LDA could easily be detected by IR or Raman spectroscopy. The Raman spectra that we collected at 77 K and 1 bar (cf. the end of the yellow arrow labeled "sample preparation" in Fig. 1(a)) only show vibrations characteristic of HDA, but no vibrations characteristic of LDA. Also the powder X-ray diffractograms that we obtained clearly show that the jump-like transformation to LDA was avoided in the course of sample preparation [14,19]. Thus, the sample that was suggested to be LDA-like and of density 0.94 g/cm$^3$ according to the interpretation provided in Ref. [2] is in fact clearly HDA and of density 1.13 g/cm$^3$.

The assumption that a liquid explores all states on its potential energy surface is very good if a liquid is studied well above its glass transition temperature, e.g., in the stable liquid state or in the supercooled state not too far below the melting temperature. This is the case for the examples mentioned in Ref. [2], in particular for polystyrene. In case of eHDA at 0.07 GPa and 140 K the sample is very close to the glass transition temperature (see Fig. 1(a), blue triangles), in the ultraviscous, deeply supercooled liquid domain. In this domain it can only explore substates within the HDA potential energy megabasin on the experimental time scale, but does not surmount the potential energy barrier corresponding to the HDA → LDA conversion. Only a "metastable equilibrium" within HDA can be reached, whereas the LDA basin remains unexplored. The LDA basin also remains unexplored during the DSC cycles, and so the endotherm observed at 116 K in DSC scans cannot be interpreted as sub-$T_g$ endotherm of LDA's glass transition.

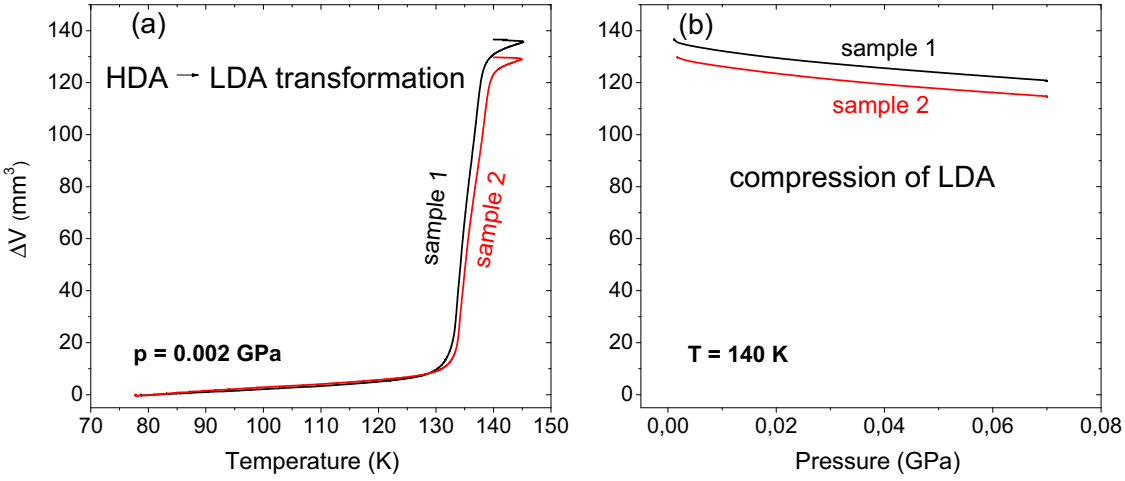


**Fig. 2.** (a) Volumetric changes $\Delta V$ incurred upon heating 600 mg of eHDA samples at 0.002 GPa to 145 K using a heating rate of 2 K/min to LDA-II. (b) Subsequent volumetric changes incurred upon compression of LDA-II at 140 K and a compression rate of 0.02 GPa/min. The solid black and the red lines refer to two different samples. (For interpretation of the references to color in figure legend, the reader is referred to the web version of the article.)

The situation would of course be very different if liquid water was compressed *at room temperature* (instead of at 140 K) to 0.07 GPa and then quenched to 77 K. At room temperature the liquid can explore all substates and upon cooling it transforms to pressure-densified LDA at <0.20 GPa and to pressure-densified HDA at >0.20 GPa (if crystallization is avoided, see the LDA-HDA equilibrium boundary in Fig. 1) [27]. If we had prepared the sample in this way, we would indeed have obtained an LDA-like sample. However, at temperatures below the crystallization line and following the yellow path in Fig. 1(a) we have obtained an eHDA sample. That is, the case of glassy polystyrene and the case of glassy water under pressure cannot be compared, and the assumption made in Ref. [2] that eHDA would transform to "pressure-densified glassy water" (resembling LDA) in the deeply supercooled regime below the crystallization temperature is at odds with the experimental findings. This removes the basis for the suggestion put forward in Ref. [2] that we have observed a sub-$T_g$ endotherm for the pressure-densified LDA-state rather than HDA's $T_g$.

## 4. One or two glass transitions in water?

Inspired by the comment's arguments [2] we performed an additional experiment, which was designed to discriminate even more clearly between the two suggested scenarios, i.e., (i) the scenario of pressure-densified glassy water and a single $T_g$ of water suggested in the comment [2] and (ii) the scenario of water polyamorphism and a double $T_g$ of water suggested by us on the basis of our experimental findings [1]. This experiment involves compression of LDA (or hyperquenched glassy water (HGW) or amorphous solid water (ASW)) to 140 K and 0.07 GPa (see yellow path in Fig. 1(b)), i.e., to the same p,T-point also reached upon decompression of HDA in our earlier experiment [1]. According to the arguments presented in Ref. [2] both LDA and HDA at 140 K and 0.07 GPa would reach the same structural state, because this p,T-point is slightly above the volumetric $T_g$ at 0.07 GPa (see Fig. 1(a)). Upon quenching to 77 K at 0.07 GPa both samples would then transform to the same material, called pressure-densified glassy water in Ref. [2]. Hence, they should also show the same DSC scan as the one reported by us as Fig. 2 in Ref. [1] (and reproduced as Fig. 1 in the comment [2]). According to our line of reasoning, we instead expect that the sample remains in the LDA state in this experiment, and accordingly we expect DSC scans similar to the DSC scans reported in the past for HGW [4], ASW [21] or LDA [5].

## 5. Experimentally discriminating between the two scenarios

When designing an experiment aimed at discriminating between the two scenarios it is important to avoid interfering crystallization effects. An LDA-sample prepared via the polyamorphic transition from eHDA was shown to be the most resistant one of the LDA type [5,28]. This type of LDA was called LDA-II [28]. Its immense resistance against crystallization was suggested to arise because it is free from hexagonal ice nanocrystals [5,17], whereas LDA samples prepared via uHDA, vapor deposition or hyperquenching might contain such nanocrystals and are hence less suitable here. Thus, we decided to employ LDA-II for the experiment described below. Following established protocols [14,19] LDA-II was prepared from eHDA, which in turn was produced by decompression of VHDA from 1.10 to 0.20 GPa at 140 K and subsequent quenching to 77 K (see yellow path in Fig. 1(b), left). The resulting eHDA sample was then heated at 0.002 GPa from 77 to 145 K at a rate of 2 K $min^{-1}$ and subsequently cooled to 140 K also at a rate of 2 K $min^{-1}$, yielding LDA-II. The LDA was compressed to 0.07 GPa at 140 K and equilibrated

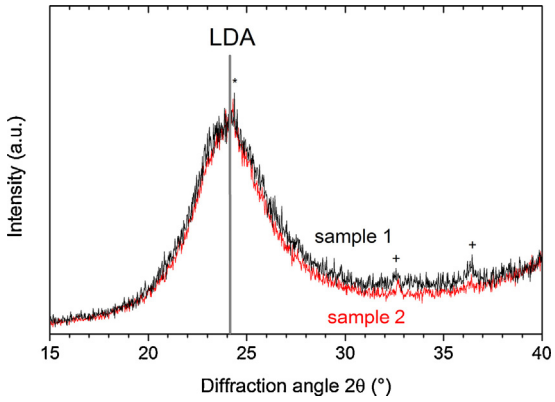


**Fig. 3.** Powder X-ray diffractograms of the samples quench-recovered from 140 K and 0.07 GPa to 77 K and 1 bar recorded in $\theta$–$\theta$ geometry at 77 K using a Siemens D5000 diffractometer (Cu-$K_{\alpha,1}$ radiation, $\lambda$ = 1.5406 Å) equipped with a Göbel mirror for parallel optics and a low-temperature Anton-Paar chamber. The vertical line marks the position of the LDA's structure factor maximum [29]. Traces of hexagonal ice $I_h$ marked by * stem from condensation on the sample from the atmosphere during sample transfer and traces of indium marked by + stem from the sample container holding the ice. (For interpretation of the references to color in figure legend, the reader is referred to the web version of the article.)

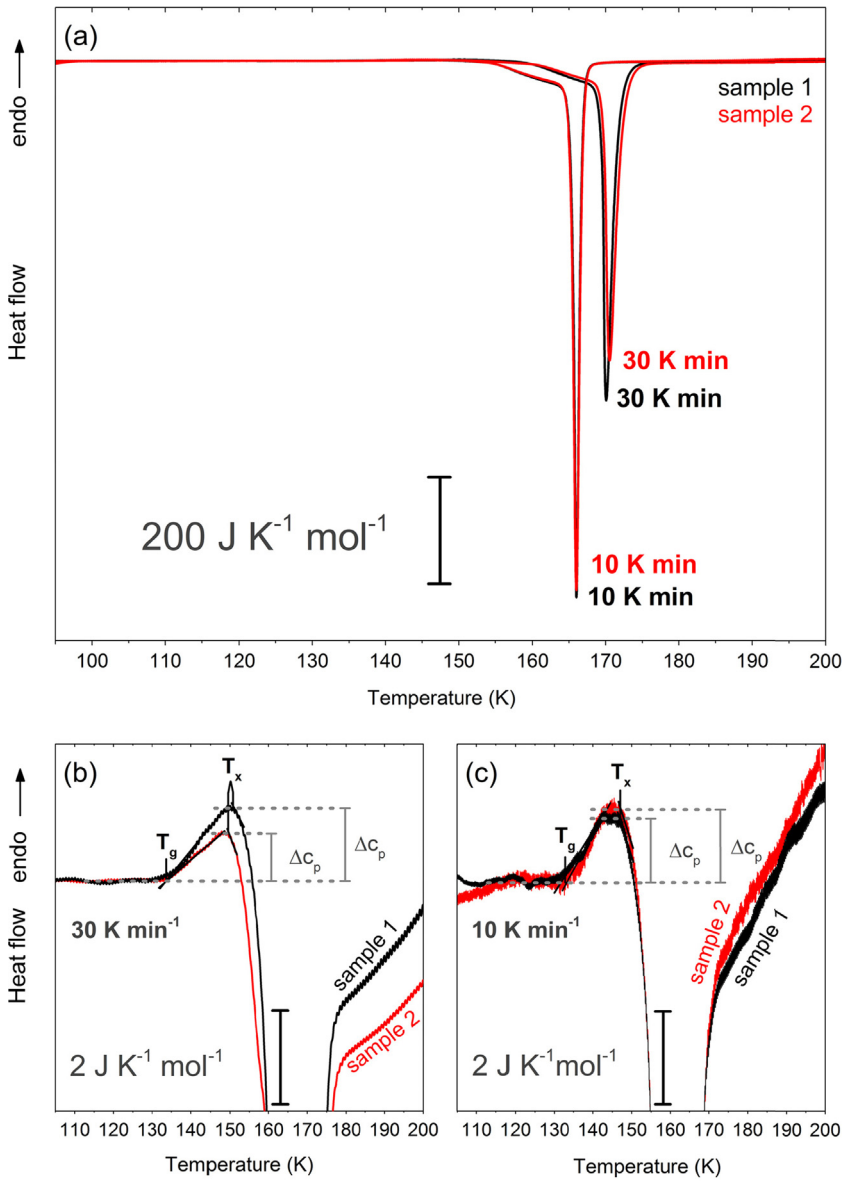


**Fig. 4.** (a) Thermograms of the quench-recovered samples recorded using about 20 mg sample in a Perkin Elmer DSC8000 at a heating rate of 30 K/min and 10 K/min. Fig. 1(b) indicates the temperature program used in the DSC study. The two samples are distinguished by their colors black and red. (b) and (c) show magnifications by a factor of 150. Onset temperatures of the glass transitions $T_g$ and onset temperatures of the crystallization to cubic ice $I_c$ $T_x$ are determined using the tangent method. Values obtained for $T_g$ and for $T_x$, as well as for the changes in heat capacity corresponding to the endotherms $\Delta C_p$ are given in Table 1. Also given in Table 1 are the values for enthalpy changes $\Delta H$ associated with the transformation to cubic ice $I_c$ shown in (a). Note that there is no massive second exotherm, which was found in our earlier work on eHDA after quench recovery from 140 K to 0.07 GPa [1], because the sample studied here is LDA and does not experience the exothermic eHDA-to-LDA transition. (For interpretation of the references to color in figure legend, the reader is referred to the web version of the article.)

for 60 s (see Fig. 1(b), middle). It was then quenched to 77 K and recovered for further analysis (see Fig. 1(b), right). The experiment and all measurements were carried out on two different sample batches to check for reproducibility (see the red and the black lines in Figs. 2–4). Fig. 2(a) shows the sudden volume change that occurs in the 130 to 140 K range when HDA is heated at 0.002 GPa. The volume change of the HDA samples (density of ≈1.13 g/cm$^3$ at 80 K and 0.002 GPa) from 80 to 145 K (see Fig. 2(a)) amounts to ≈140 mm$^3$ (or ≈130 mm$^3$ for a second sample). Both samples comprised initially 600 mm$^3$ liquid water (density of ≈1.00 g/cm$^3$ at 298 K and 1 bar). About 15% of the change in volume can be attributed to thermal expansion, whereas about 85% correspond to the sudden volume expansion upon transformation from HDA to LDA. When compressed from 0.002 GPa to 0.07 GPa at 140 K and

**Table 1**
Calorimetric data obtained by the evaluation of the thermograms shown in Fig. 4.

| | Heating rate (K/min) | $\Delta C_p$ (J K$^{-1}$ mol$^{-1}$) | $\Delta H$ (J mol$^{-1}$) | $T_g$ (K) | $T_x$ (K) |
|---|---|---|---|---|---|
| Sample 1 | 30 | 1.59 | −1367 | 134 | 151 |
| Sample 2 | 30 | 1.04 | −1434 | 134 | 150 |
| Sample 1 | 10 | 1.40 | −1389 | 133 | 147 |
| Sample 2 | 10 | 1.61 | −1402 | 133 | 147 |

cooled at a moderately low rate of 0.02 GPa/min (see Fig. 2(b)), the samples' volume changes by about −20 mm$^3$, reflecting the isothermal compressibility of the low-density ice plus the isothermal compressibility of the metal pistons used in the piston-cylinder setup.

From the data in Fig. 2(b) one clearly recognizes that there is no back-transformation to HDA: The powder X-ray diffractograms recorded on the quench-recovered ice at 77 K and 1 bar show a rather broad halo peak at about 24° which confirms the amorphous character of the samples (Fig. 3). The halo-peak is shifted by about 5° compared to the HDA halo peak observed in our earlier work [1], and exactly matches the known halo position for LDA [29]. Further characterization of the samples was carried out using DSC, employing heating rates of 10 K/min (see Fig. 4(a)) and 30 K/min (see Fig. 4(b)). The thermograms depicted in these figures reveal one single massive exotherm. This exotherm indicates crystallization of LDA to cubic ice. Thus, also the thermogram confirms the LDA nature of the sample. The exotherm can be quantified by comparing it with the area of the melting peak. The latent heat released above ≈150 K upon crystallization of LDA is on average −1.4 kJ mol$^{-1}$ which is close to the value of −1.3 kJ mol$^{-1}$ obtained by Elsaesser et al. [5]. The DSC scans show signatures characteristic of glass transitions involving a $C_p$ increase of about 1.0–1.6 J K$^{-1}$ mol$^{-1}$, which is again similar to the values obtained by Elsaesser et al. [5]. The heat capacity increase is terminated prematurely, i.e., by the large exotherm indicating the crystallization to cubic ice (see Fig. 4(a)) [5]. The observation of an incomplete heat capacity step is well known from earlier DSC studies on LDA, ASW and HGW [4,5,21]. The change in heat capacity at the LDA glass transition is much less than the 4.8 J K$^{-1}$ mol$^{-1}$ increase at water's second glass transition near 116 K pertaining to HDA [1].

In order to discriminate between the alternative scenarios (i) and (ii), formulated near the end of Section 4, it is important to observe that the DSC scans shown in Fig. 4 differ from the DSC scans of eHDA reported earlier [1]: The data in Fig. 4 – which was obtained using the modified protocol – clearly demonstrate that there is only a single massive exotherm, indicating crystallization of LDA to cubic ice. As mentioned above this exotherm is very much different in magnitude compared to the local minima observed for pressure densified glasses (polysterene, see Fig. 2 in Ref. [2]). In Ref. [2] the local endothermic maximum associated with a sub-$T_g$ has almost the same magnitude as the following local exothermic minimum. In the case of LDA the endothermic feature starting at $T_g$ is considerably smaller than the LDA → I$_c$ transition exotherm (by a factor of approximately 1000 for heating rates of 10 K/min and a factor of approximately 600 for 30 K min$^{-1}$). Conversely, following the original protocol [1] two massive exotherms are observed, indicating the polyamorphic HDA → LDA transition (first exotherm) *and* the crystallization to cubic ice (second exotherm). These differences, together with the evidence from the X-ray diffractograms (Fig. 3) and the thermograms (Fig. 4) and with the findings reported earlier by us [1], demonstrate that the two samples quench-recovered from 0.07 GPa to 140 K are clearly distinct: The ones studied in Ref. [1] are eHDA and the others, studied here, are in fact LDA. These results clearly support the case for water's polyamorphism and metastability as sketched in Fig. 1. On this basis, designating these samples both as pressure-densified glassy water is not justified. We thus reiterate that we do not see an alternative to interpreting the two glass transitions as two distinct phenomena, linking two distinct amorphous ices to two distinct ultraviscous liquids.

## 6. Dielectric spectroscopy

In Ref. [2] concerns were expressed which cast doubt on the reliability of the dielectric data presented in our work [1]. For instance,

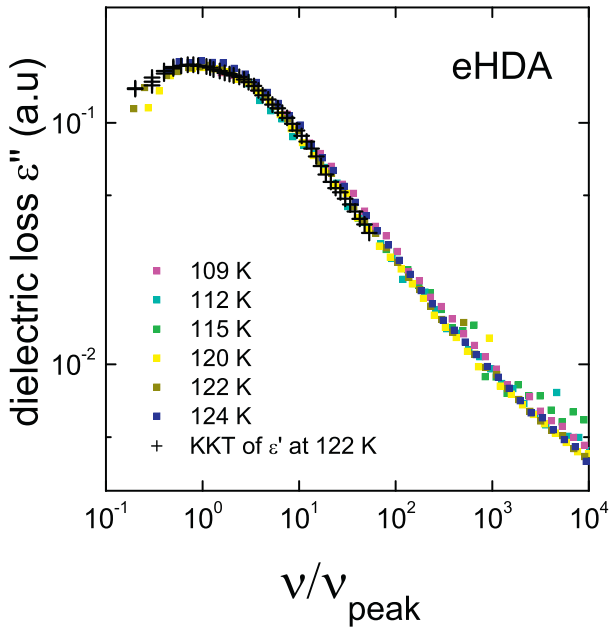


**Fig. 5.** Dielectric loss recorded in the high-density state of ultraviscous water taken from Ref. [1] and re-plotted on a reduced frequency scale. In the peak region the data reveal a common shape in this master plot, thereby demonstrating that shape and amplitude of the relaxation spectra are temperature independent. The agreement of the dielectric loss data (imaginary part of $\varepsilon^*$) with those from a Kramers–Kronig transformation (KKT) of the real part of $\varepsilon^*$ demonstrates that our data was taken in the linear-response regime.

it was stated that "the experimental procedure and data analysis of the dielectric relaxation study is too inaccurate to reliably support the view that water has a second $T_g$" [2]. This judgment with which we do not agree suggests that in our work not all necessary checks were made, in particular when determining the relaxation time of the various ices as precisely as possible. As will become clear in the following this is not the case.

In our study the statement "a standard procedure" was used to motivate that the dielectric relaxation times were obtained by time-temperature superposition (TTS). Indeed TTS is not always applicable and therefore needs to be checked carefully. To demonstrate the applicability of TTS in the present context, in Fig. 5 we present the data on eHDA from Ref. [1] as an example. After shifting these data along the frequency axis one recognizes that the spectral shape remains temperature invariant and that no further adjustments are necessary to obtain almost perfect agreement in the region of the main peak. In view of the relatively narrow temperature range in which the spectra were collected it is barely surprising that a change in the distribution of relaxation times and/or the dielectric relaxation strength is not observable, i.e., the simple scaling procedure that we just described works without yielding hints for temperature dependent changes of relaxation strength. Fig. 5 reveals slight deviations from TTS at the largest scaled frequencies $\nu/\nu_{peak}$ which, however, do not at all impede a reliable determination of the peak frequencies $\nu_{peak}$ and thus of the corresponding time constants.

Then, under the heading "Questionable reliability of the dielectric spectra", in Ref. [2] further issues are listed in seven items. However, only item (i) and its iteration in items (ii) and (iii) questions the reliability of our dielectric data. The remaining items do not really refer to our data as such but are mere comments or ask for additional information which we are happy to provide.

In items (i) and (ii) it is stated that incomplete capacitor filling can render the experimentally observed relaxation times shorter than they in fact are. In Ref. [2] item (iii) simply restates this point.

Being aware that under certain circumstances an accurate determination of relaxation times is not straightforward [30], we alerted the reader of the incomplete filling of our sample capacitor. Incomplete capacitor filling can additionally arise from a simple shrinking of the specimen within its (fixed) capacitor gap due to thermal contraction. The consequent occurrence of an (empty) capacitance in series with that stemming from the sample is at the basis of the estimate provided by Gough et al. [31] to which Ref. [2] refers.

However, this latter scenario of serial capacitors does not adequately capture the present experimental situation. In our case incomplete filling means that the void space, arising from the powdering of our samples (which is taken to have a 'true' complex dielectric permittivity $\varepsilon^*$), is dispersed spatially in an overall more or less homogenous fashion within the sample capacitor, akin to the situation discussed in Ref. [32]. The scenario discussed in that work when applied to the present case just implies that not all of the void space appears as either parallel or else as serial empty capacitance but as an isotropically properly weighted distribution thereof.

Reasonably assuming $\varepsilon^*_{\text{void}} = 1$ for the dielectric constant of void space and designating $y$ as the overall filling factor of the capacitor, Eq. (2) in Ref. [32] yields $\varepsilon^*_{\text{exp}} = (2/3)y/\varepsilon^* + (1/3)y\varepsilon^* + 1 - y$ for the experimentally determined complex dielectric permittivity. With the magnitude of $\varepsilon^*$ in amorphous ices very much larger than 1 [33,34] it is clear that the first term on the right hand side of the given equation can be neglected, even if the filling factor would be low. Hence, for all practical purposes only the amplitude of the complex dielectric permittivity is affected and, in particular, these considerations show that the determination of relaxation times applied in Ref. [1] is reliable under the provisos pointed out above.

It is well known that impurity doping can affect the relaxation times in ices significantly and we fully agree with the statement in item (ii) that "it is doubtful that . . . the amorphous and crystalline ices can be identified by such experiments". However, no such claim was advanced in Ref. [1] where in view of the ices relevant for our study we noted that "the ice $I_c$, LDL, and HDL phases are clearly distinguishable solely on the basis of their relaxation time traces" where the word "phase" seems appropriate only for ice I and should have been replaced by the word "state" when referring to high-density liquid water (HDL) and LDL.

With respect to items (iv) and (v) we can say that in our study we used samples produced from several preparation batches. None of them was intentionally doped. Hence, the number of unavoidable intrinsic defects should be similar in all amorphous and crystalline ices that we dealt with in our study. For this statement to apply it has to be ascertained that during the experiment the vast majority of defects remains inside the sample interior. In turn this requires that the defects' translational diffusion coefficient, which we estimate in the following, is sufficiently small.

For the effective cooling rates implied by our study (10 min for a frequency sweep and 4–5 min between subsequent measurements, each 2 K apart) transformation to, e.g., cubic ice occurs at a temperature at which the relaxation frequency is $\nu \approx 1/(2\pi \times 0.1\,\text{s})$. In lack of suitable experimental data or better assumptions, to provide a conservative estimate we interpret this frequency *entirely* as a translational jump rate, but we point out that for several glass formers a decoupling of rotational and translational degrees of freedom may exist [35].

Nevertheless assuming a rate $\nu$ as just described and taking the jump distance as $a = 2$ Å, one estimates a diffusion coefficient of $D = a^2\nu/6 \approx 10^{-20}\,\text{m}^2/\text{s}$. The total time our LDL sample was subjected to temperatures between the glass transition and the transformation to the cubic phase did not exceed about $t = 9000$ s. This time interval $t$ thus provides the maximum total diffusion time and a conservative estimate for the maximum mean-square displacement is $\langle r^2\rangle < 6Dt \approx 6 \times 10^{-16}\,\text{m}^2$. At the transformation temperature the resulting mean displacement of about $\sqrt{\langle r^2\rangle} < 25$ nm is much smaller than the typical grain sizes relevant for our experiments. Therefore, the number of (intrinsic) defects in our samples is not expected to change in the course of these dielectric experiments.

Item (vi) asks for reasons why our samples "remain[s] in equilibrium at 124 K for a period of at least 10 min to allow collection of the isothermal spectra." The answer is that in preliminary experiments addressing the kinetics of the transition from the HDL to the LDL state we found that not even a partial transformation could be discerned from the data so that obviously this transition proceeds sufficiently slowly. Details of the transformation kinetics were not within the scope of Ref. [1] and will be reported elsewhere.

Finally, in item (vii) of Ref. [2] it is pointed out that "Calorimetric relaxation involves fluctuations of density and structural order, while dielectric relaxation involves fluctuation of only the dipole vector and these two fluctuations are not the same." Viewed from that perspective the (near) coincidence of relaxation times determined from these different experimental techniques (see Fig. 4 in Ref. [1]), despite being often observed in studies of glass formers in general, is far from trivial. Therefore, it is reassuring that concurrent evidence for the existence of two glass transitions in amorphous waters was obtained by calorimetry and additionally by dielectric spectroscopy, two techniques which really offer quite different perspectives on the dynamics of the materials under study.

To compare the time constants resulting from dielectric spectroscopy on the high- and low-density samples with those from rate dependent DSC results, we used the well-established relation according to which the calorimetric relaxation time is inversely proportional to the scanning rate, $|q|$. From previous work, we are fully aware of the fact that the exact proportionality constant relating rate and relaxation time may depend on a range of different factors such as the nonexponentiality and the nonlinearity of the structural relaxation [36]. Hence, the proportionality constants in the phenomenological relations as expressed in Ref. [37] or by the version used in our work [1] – which is criticized in Section 5.2 of [2] – can only be viewed as approximations. Nevertheless, it is hard to believe that the agreement between the calorimetrically and dielectrically determined time constants which is excellent for the high-density as well as for the low-density samples (see Fig, 4 in Ref. [1]) is purely accidental. In any case, and independent of any specific proportionality factor, from frequency dependent dielectric spectroscopy and from rate dependent calorimetry the same effective energy barrier is obtained for the relaxation in the high-density liquid [1].

Finally, in Ref. [2] it is questioned that the Kramers–Kronig relation, which is based on the general conditions of causality and linearity of the response [38] is fulfilled by the dielectric data presented in our work [1]. To check whether the Kramers–Kronig relation indeed applies here and to minimize potential uncertainties in the transformation procedure, we considered data which display a well-resolved dispersion step in the real part, $\varepsilon'$, of the dielectric constant and a corresponding loss peak, $\varepsilon''$, in the experimentally accessible frequency window. Using the numerical transformation procedure based on [39] and described in more detail in Ref. [40] we calculated $\varepsilon''(\nu)$ from $\varepsilon'(\nu)$ and show the results obtained for $T = 122$ K as crosses in Fig. 5. One recognizes that the calculated and the experimentally recorded dielectric loss spectra nicely agree. This demonstrates compatibility of our data with the Kramers–Kronig relation. Owing to the structure of this relation the requested check does not allow one to make any statements regarding the absolute value of the high-frequency dielectric constant, $\varepsilon_\infty$.

With respect to the remarks near the end of Section 5.3 in Ref. [2] we summarize the response to the criticism on the dielectric part

of our work as follows: (a) the incomplete capacitor filling clearly stated in Ref. [1] is of negligible importance for the determination of relaxation times, (b) the equilibrium permittivity is constant in the limited temperature range of our study, and (c) consistency with the Kramers–Kronig relation is demonstrated.

## 7. Conclusion

In summary, we do not see any evidence that would necessitate a reinterpretation of our work. In fact, the new data recorded here on the basis of the experimental protocol inspired by the suggestions in Ref. [2] strengthens the case of water's second glass transition, water polyamorphism, and the observation of two distinct, deeply supercooled liquids of water differing by about 25% in density.

## Acknowledgements

We are thankful to the Austrian Science Fund FWF (START award Y391 and project I1392) and the Alexander von Humboldt Foundation (Friedrich Wilhelm Bessel award to T.L.) for financial support. Work at the Technische Universität Dortmund was supported by the Deutsche Forschungsgemeinschaft.

## References

[1] K. Amann-Winkel, C. Gainaru, P.H. Handle, M. Seidl, H. Nelson, R. Böhmer, T. Loerting, Water's second glass transition, Proc. Natl. Acad. Sci. U. S. A. 110 (2013) 17720–17725.
[2] G.P. Johari, Comment on "Water's second glass transition' and the sub-$T_g$ features of pressure-densified glasses", Thermochim. Acta (2015), http://dx.doi.org/10.1016/j.tca.2015.01.024 (in press).
[3] D.T. Limmer, D. Chandler, Theory of amorphous ices, Proc. Natl. Acad. Sci. U. S. A. 111 (2014) 9413–9418.
[4] G.P. Johari, A. Hallbrucker, E. Mayer, The glass → liquid transition of hyperquenched water, Nature 330 (1987) 552–553.
[5] M.S. Elsaesser, K. Winkel, E. Mayer, T. Loerting, Reversibility and isotope effect of the calorimetric glass → liquid transition of low-density amorphous ice, Phys. Chem. Chem. Phys. 12 (2010) 708–712.
[6] Y. Yue, C.A. Angell, Clarifying the glass-transition behaviour of water by comparison with hyperquenched inorganic glasses, Nature 427 (2004) 717–720.
[7] N. Giovambattista, C.A. Angell, F. Sciortino, H.E. Stanley, Glass-transition temperature of water: a simulation study, Phys. Rev. Lett. 93 (2004) 047801.
[8] I. Kohl, L. Bachmann, E. Mayer, A. Hallbrucker, T. Loerting, Water behaviour: glass transition in hyperquenched water? Nature 435 (2005) E1.
[9] C.A. Angell, Glass transition dynamics in water and other tetrahedral liquids: 'order-disorder' transitions versus 'normal' glass transitions, J. Phys.: Condens. Matter 19 (2007) 205112.
[10] T. Loerting, V.V. Brazhkin, T. Morishita, Multiple amorphous-amorphous transitions, Adv. Chem. Phys. 143 (2009) 29–82.
[11] K. Amann-Winkel, R. Böhmer, F. Fujara, C. Gainaru, B. Geil, T. Loerting, Water's controversial glass transitions, Rev. Mod. Phys. (2015) (submitted for publication).
[12] O. Mishima, Reversible first-order transition between two $H_2O$ amorphs at ≈0.2 GPa and ≈135 K, J. Chem. Phys. 100 (1994) 5910–5912.
[13] E.L. Gromnitskaya, O.V. Stal'gorova, V.V. Brazhkin, A.G. Lyapin, Ultrasonic study of the nonequilibrium pressure–temperature diagram of $H_2O$ ice, Phys. Rev. B 64 (2001) 094205.
[14] K. Winkel, E. Mayer, T. Loerting, Equilibrated high-density amorphous ice and its first-order transition to the low-density form, J. Phys. Chem. B 115 (2011) 14141–14148.
[15] O. Mishima, L.D. Calvert, E. Whalley, "Melting ice I" at 77 K and 10 kbar: a new method of making amorphous solids, Nature 310 (1984) 393–395.
[16] R.J. Nelmes, J.S. Loveday, T. Strässle, C.L. Bull, M. Guthrie, G. Hamel, S. Klotz, Annealed high-density amorphous ice under pressure, Nat. Phys. 2 (2006) 414–418.
[17] M. Seidl, K. Amann-Winkel, P.H. Handle, G. Zifferer, T. Loerting, From parallel to single crystallization kinetics in high-density amorphous ice, Phys. Rev. B 88 (2013) 174105.
[18] M. Seidl, A. Fayter, J.N. Stern, G. Zifferer, T. Loerting, Shrinking water's no man's land by lifting its low-temperature boundary, Phys. Rev. B 91 (2015) 144201.
[19] K. Winkel, M.S. Elsaesser, E. Mayer, T. Loerting, Water polyamorphism: reversibility and (dis)continuity, J. Chem. Phys. 128 (2008) 044510.
[20] T. Loerting, M. Bauer, I. Kohl, K. Watschinger, K. Winkel, E. Mayer, Cryoflotation: densities of amorphous and crystalline ices, J. Phys. Chem. B 115 (2011) 14167–14175.
[21] A. Hallbrucker, E. Mayer, G.P. Johari, Glass–liquid transition and the enthalpy of devitrification of annealed vapor-deposited amorphous solid water: a comparison with hyperquenched glassy water, J. Phys. Chem. 93 (1989) 4986–4990.
[22] E. Whalley, High-density amorphous ice made by "melting" ice I or low-density amorphous ice at 77 K, Physica B+C (Amsterdam) 139–140 (1986) 314–318.
[23] E. Whalley, D.D. Klug, M.A. Floriano, E.C. Svensson, V.F. Sears, Recent work on high-density amorphous ice, J. Phys. Colloq. C1 (1987) 429–434.
[24] H.R. Pruppacher, J.D. Klett, Microphysics of Clouds and Precipitation, D. Reidel, Dordrecht, 1980.
[25] M. Seidl, M.S. Elsaesser, K. Winkel, G. Zifferer, E. Mayer, T. Loerting, Volumetric study consistent with a glass-to-liquid transition in amorphous ices under pressure, Phys. Rev. B 83 (2011) 100201.
[26] T. Loerting, C. Salzmann, I. Kohl, E. Mayer, A. Hallbrucker, A second distinct structural "state" of high-density amorphous ice at 77 K and 1 bar, Phys. Chem. Chem. Phys. 3 (2001) 5355–5357.
[27] O. Mishima, Y. Suzuki, Vitrification of emulsified liquid water under pressure, J. Chem. Phys. 115 (2001) 4199–4202.
[28] K. Winkel, D.T. Bowron, T. Loerting, E. Mayer, J.L. Finney, Relaxation effects in low density amorphous ice: two distinct structural states observed by neutron diffraction, J. Chem. Phys. 130 (2009) 204502.
[29] T. Loerting, N. Giovambattista, Amorphous ices: experiments and numerical simulations, J. Phys.: Condens. Matter 18 (2006) R919–R977.
[30] C.P. Gainaru, R. Böhmer, Comment on "Hidden slow dynamics in water", Phys. Rev. Lett. 104 (2010) 249803.
[31] S.R. Gough, E. Whalley, D.W. Davidson, Dielectric properties of the hydrates of argon and nitrogen, Can. J. Chem. 46 (1968) 1673–1681.
[32] A. Fillmer, C. Gainaru, R. Böhmer, Broadened dielectric loss spectra and reduced dispersion strength of viscous glycerol in a connective tissue protein, J. Non-Cryst. Solids 356 (2010) 743–746.
[33] O. Andersson, A. Inaba, Dielectric properties of high-density amorphous ice under pressure, Phys. Rev. B 74 (2006) 184201.
[34] O. Andersson, Dielectric relaxation of the amorphous ices, J. Phys.: Condens. Matter 20 (2008) 244115.
[35] I. Chang, H. Sillescu, Heterogeneity at the glass transition: translational and rotational self-diffusion, J. Phys. Chem. B 101 (1997) 8794–8801.
[36] A. Pimenov, R. Böhmer, A. Loidl, Relaxation times at the rate-dependent glass transition, Prog. Theor. Phys. Suppl. 126 (1997) 185–190.
[37] I.M. Hodge, Enthalpy relaxation and recovery in amorphous materials, J. Non-Cryst. Solids 169 (1994) 211–266.
[38] C.J.F. Böttcher, P. Bordewijk, Theory of Electric Polarization. Volume II: Dielectrics in Time-Dependent Fields, Elsevier, Amsterdam, 1978.
[39] A.K. Jonscher, Dielectric Relaxation in Solids, Chelsea, London, 1983.
[40] C. Gainaru, R. Böhmer, G. Williams, Ion sweeping in conducting dielectric materials, Eur. Phys. J. B 75 (2010) 209–216.